

Kilo-Gauss Magnetic Fields in Three DA White Dwarfs

R. Aznar Cuadrado,¹ S. Jordan,² R. Napiwotzki,³ H. M. Schmid,⁴
S. K. Solanki,¹ and G. Mathys⁵

¹*Max-Planck-Institut für Sonnensystemforschung, Max-Planck-Str. 2,
37191 Katlenburg-Lindau, Germany*

²*Astronomisches Rechen-Institut, Mönchhofstr. 12-14, 69120
Heidelberg, Germany*

³*Department of Physics & Astronomy, University of Leicester,
University Road, Leicester LE1 7RH, UK*

⁴*Institut für Astronomie, ETH Zentrum, 8092 Zürich, Switzerland*

⁵*European Southern Observatory, Casilla 19001, Santiago 19, Chile*

Abstract. We have detected longitudinal magnetic fields between 2 and 4 kG in three normal DA white dwarfs (WD 0446–790, WD 1105–048, WD 2359–434) out of a sample of 12 by using optical spectropolarimetry done with the VLT Antu 8 m telescope equipped with FORS1. With the exception of 40 Eri B (4 kG) these are the first positive detections of magnetic fields in white dwarfs below 30 kG. A detection rate of 25 % (3/12) may indicate now for the first time that a substantial fraction of white dwarfs have weak magnetic fields. This result, if confirmed by future observations, would form a cornerstone for our understanding of the evolution of stellar magnetic fields.

1. Introduction

On the main sequence and at later stages of evolution, magnetic fields have a major impact on the angular momentum loss and stellar winds, on building-up chemical anomalies and abundance inhomogeneities across the stellar surface, on convection and the related coronal activity, and other evolutionary processes especially in interacting binaries. The first detection of a magnetic field on a white dwarf (WD) was made by Kemp et al. (1970) on Grw+70° 8247, and large spectroscopic and polarimetric surveys have been carried out since then (e.g. Schmidt & Smith 1995). The magnetic fields of WDs could simply be “fossil” remnants of the fields already present in main-sequence stars, but strongly amplified by contraction. This hypothesis assumes that the magnetic flux (e.g. through the magnetic equator) is conserved to a large extent during the stellar evolution.

In main-sequence stars magnetic fields have been detected directly mainly for peculiar magnetic Ap and Bp stars with rather well organized fields and field strengths $\sim 10^2 - 10^4$ G. For weak fields in A to O stars ($B < 10^2$ G) direct magnetic field detections are still very rare. For sun-like stars ample evidence (coronal activity) for the presence of complicated small-scale fields exists, but direct measurements are only possible for the more active stars (e.g. Saar 1996; Rüedi et al. 1997). The contraction to a WD amplifies the magnetic fields by

about 4 orders of magnitude, so that weak and often undetectable magnetic fields on the main sequence become measurable during the WD phase. This is supported by the known magnetic WDs with Megagauss fields ($B = 10^6 - 10^9$ G). Their frequency and spatial distribution, as well as their masses, are consistent with the widely accepted view that they are the descendents of the magnetic Ap and Bp stars (e.g. Mathys 2001). Magnetic main-sequence stars with weaker magnetic fields have been suggested as possible progenitor candidates for the magnetic degenerates with weaker fields (e.g. Schmidt et al. 2003). The B stars on which weaker fields have been detected may be the missing stars. However, even the most sensitive observations are limited to some tens of Gauss on main-sequence stars.

Thus, magnetic field amplification during stellar evolution may offer the opportunity to investigate ~ 1 G magnetic fields (averaged global fields) in normal main-sequence stars with observations of ~ 1 kG magnetic fields during the WD stage. Zeeman splitting of narrow NLTE line cores in the Balmer lines becomes undetectable in intensity spectra for weak fields (< 20 kG) or for objects without narrow line core. Therefore, spectropolarimetry is the most promising technique for successful detections of weak magnetic fields.

It is interesting to note that, recently, magnetic fields have also been detected in the direct progeny of white dwarfs, subdwarfs and central stars of planetary nebulae (O'Toole et al. and Jordan et al., these proceedings).

2. Observations and Data Reduction

Spectropolarimetric observations of a sample of 12 normal DA WDs were carried out during the period 4 November 2002 – 3 March 2003, in service mode by ESO staff members using FORS1 at the VLT. With a $0.8''$ wide slit we obtained a (FWHM) spectral resolution of 4.5 \AA . The data were recorded using a Tek. 2048×2048 CCD with $24 \mu\text{m}$ pixels which correspond to a pixel scale of $0.2''/\text{pixel}$ in spatial and $1 \text{ \AA}/\text{pixel}$ in spectral direction. Spectra were acquired with grism G600B (spectral range $3400 - 6000 \text{ \AA}$), covering all H I Balmer lines from $H\beta$ to the Balmer jump simultaneously.

Our 12 targets were selected with the criterion of not showing any sign of Zeeman splitting visible in the SPY-UVES spectra (Napiwotzki et al. 2003), and hence no magnetic fields above a level of about 20 kG. All our targets have strong hydrogen lines, ideal for measuring line polarisation, and no bright companions. Most of our targets were observed in at least two nights.

In all frames the bias level was subtracted and the frames were cleaned of cosmic ray hits. The frames were then flat-field corrected and the wavelength calibration was applied.

3. Circular Polarisation

In order to obtain circular polarisation spectra a Wollaston prism and a quarter-wave plate were inserted into the optical path. Each exposure yields two spectra on the detector, one from the extra-ordinary beam and the other from the ordinary beam. Stokes V is obtained from a differential measurement of photon

counts in either the ordinary or extra-ordinary beams, measured at two different angles of the retarder waveplate. We adopted the FORS1 standard observing sequence for circular polarimetry consisting of exposures with retarder plate position angles $+45^\circ$ and -45° .

In order to derive the circular polarisation from a sequence of exposures, we added up the exposures with the same quarter-wave plate position angle. The Stokes (V/I) can be obtained as

$$\frac{V}{I} = \frac{(R-1)}{(R+1)}, \quad \text{with } R^2 = \left(\frac{f_o}{f_e}\right)_{\alpha=+45} \times \left(\frac{f_e}{f_o}\right)_{\alpha=-45} \quad (1)$$

where V is the Stokes parameter which describes the net circular polarisation, I is the unpolarized intensity, α indicates the nominal value of the position angle of the retarder waveplate, and f_o and f_e are the fluxes on the detector from the ordinary and extra-ordinary beams of the Wollaston, respectively.

4. Determination of Weak Magnetic Fields

For field strengths below 10 kG the Zeeman splitting of the Balmer lines is less than 0.1 Å. This is well below the width of the cores of the Balmer lines in all the stars of our sample (typically a few Å). Therefore, we can apply the weak-field approximation (e.g., Landi degl'Innocenti & Landi degl'Innocenti 1973) without any loss of accuracy. According to this approximation the measured V and I profiles are related to $\langle B_z \rangle$ by the expression:

$$\frac{V}{I} = -g_{eff} C_z \lambda^2 \frac{1}{I} \frac{\partial I}{\partial \lambda} \langle B_z \rangle, \quad (2)$$

where g_{eff} is the effective Landé factor ($= 1$ for all hydrogen lines of any series, Casini & Landi degl'Innocenti 1994), λ is the wavelength expressed in Å, $\langle B_z \rangle$ is the mean longitudinal component of the magnetic field expressed in Gauss and the constant $C_z = e/(4\pi m_e c^2)$ ($\simeq 4.67 \times 10^{-13} \text{ G}^{-1} \text{ Å}^{-1}$). Note that this approximation also holds if instrumental broadening is present, but it is not generally correct if the profiles are rotationally broadened (Landstreet 1982).

The error associated with the determination of the longitudinal field obtained from individual Balmer lines is larger for Balmer lines at shorter wavelengths than for lines at longer wavelengths. This is due to the combination of two effects: while the Zeeman effect increases as lambda squared, most other line broadening effects depend linearly on lambda, so that the magnetic field is better detected at longer wavelengths than at shorter wavelengths; furthermore, the Balmer lines at shorter wavelengths are less deep, so that $\partial I/\partial \lambda$ is smaller. Using H β and H γ simultaneously, we obtained a determination of the mean longitudinal magnetic field that best fit the observed (V/I).

For stars observed during more than one night the circular polarisation spectra (V/I) flux weighted means were calculated. The averaging helps to extract signal hidden in the noise of the individual exposures if the stellar Zeeman signal remains unchanged with time. In two of the averaged spectra (corresponding to WD 0446–789, see Fig. 1, and WD 2359–434) a moderate S-shape circular

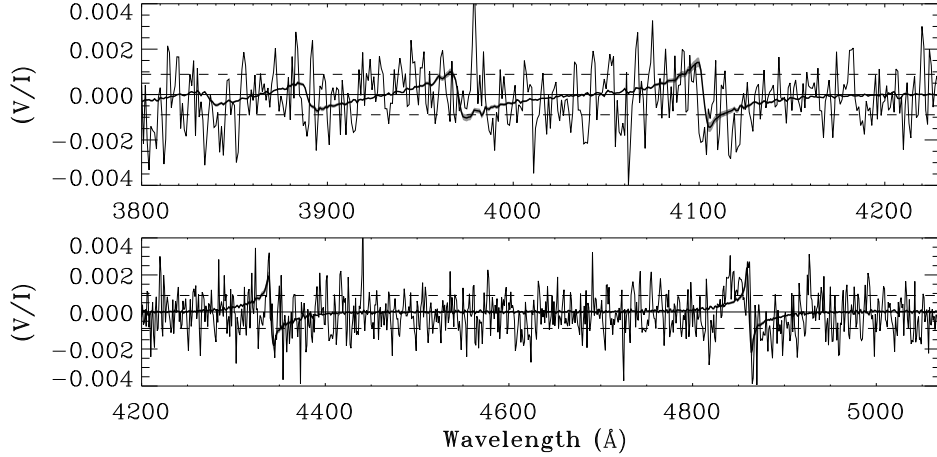


Figure 1. (V/I) spectra of WD 0446–789 (thin solid line) in the region of $H\beta$ and $H\gamma$ (bottom) and close to the Balmer jump (top). The solid horizontal line indicates the zero level. The horizontal dashed lines indicate the position of the 1σ level of the average (V/I) spectrum. The light shading represents the variation between (V/I) spectra predicted by the low-field approximation (Eq. 2) using B values of 4283 ± 640 G (thick solid line).

polarisation signature across $H\beta$ and $H\gamma$ can be noticed. For WD 1105–048 polarisation reversals of those lines were only present in one of the two observing nights. This may indicate a different orientation of the magnetic field between the two epochs due to stellar rotation.

To determine the longitudinal component of the magnetic field for each measurement we compared the observed circular polarisation for an interval of ± 20 Å around $H\beta$ and $H\gamma$ with the prediction of Eq. 2. The best fit for $\langle B_z \rangle$, the only free parameter, was found by a χ^2 -minimisation procedure. If we assume that no magnetic field is present, all deviations from zero polarization are due to noise. This can be expressed by the standard deviation σ over the respective intervals around the Balmer lines. In Table 1 the best fits for B_z derived from the analysis of $H\beta$ and $H\gamma$ lines are shown. We find a significant magnetic field in WD 2359–434, WD 0446–789 (see Fig. 1) and WD 1105–048. For the first two stars the magnetic field is detected at the 3σ level individually from $H\beta$ and $H\gamma$, as well as from the combination of both lines. Higher members of the Balmer series do not contain enough V -signal to give reliable results, but the analysis of $H\delta$ confirms our positive detections of magnetic fields.

5. Atmospheric and Stellar Parameters

Masses and cooling ages of WDs are of special interest to distinguish between the proposed formation scenarios. These quantities can be computed from the fundamental stellar parameters temperature and gravity, which can be derived by a model atmosphere analysis of the spectra, and theoretical cooling tracks.

Table 1. Fitted parameters of the three WDs with positive detections of magnetic fields.

WD	T_{eff} [kK]	$\log g$ [cgs]	M [M_{\odot}]	$d(\text{spec})$ [pc]	t_{cool} [Myr]	B_z [G]
0446–789	23.45	7.72	0.49	48.8	21	4283±640
1105–048	15.28	7.83	0.52	24.5	142	–2134±447
2359–434	8.66	8.56	0.95	—	2200	–3138±422

The observed line profiles are fitted with theoretical spectra from a large grid of NLTE spectra calculated with the code developed by Werner (1986).

The observed and theoretical Balmer line profiles are normalised to a linear continuum in a consistent manner. Radial velocity offsets are corrected by shifting the spectra to a common wavelength scale. The synthetic spectra are convolved to the resolution of the observed spectra (4.5 Å) with a Gaussian and interpolated to the actual parameters. The atmospheric parameters are then determined by minimising the χ^2 value by means of a Levenberg-Marquardt steepest descent algorithm. This procedure is applied simultaneously to all Balmer lines of one observed spectrum. Errors are estimated to be 2.3% in T_{eff} and 0.07 dex in $\log g$ (Napiwotzki et al. 1999).

The parameters listed in Table 1 are the averages of the fit results for the individual spectra. WD masses were computed from a comparison of parameters derived from the fit with the grid of WD cooling sequences of Benvenuto & Althaus (1999) for an envelope hydrogen mass of $10^{-4}M_{\text{WD}}$. Spectroscopic distances $d(\text{spec})$ are determined from the absolute magnitudes computed for the given stellar parameters using the synthetic V band fluxes computed by Bergeron et al. (1995) and the V magnitudes of the stars. The agreement between our results and values collected from the literature is generally good.

6. Discussion and Conclusions

Three stars out of 12 normal DA WDs of our sample, WD 0446-789, WD 1105-048 and WD 2359-434, exhibit magnetic fields of a few kilogauss in one or all available observations. The detection rate of 25 % suggests strongly that a substantial fraction of WDs have weak magnetic fields.

With the exception of the bright WD 40 Eri B, for which a magnetic field of only 4 kG had been detected (Fabrika et al. 2003), our three detections have the weakest magnetic fields discovered so far in white dwarfs. Our investigation is based on the averaged longitudinal component of the magnetic field, meaning that the maximum magnetic field at the WD surface can be stronger, depending on the field geometry and on the orientation relative to the observer. Therefore, our results for the three objects with a positive detection are lower limits, since cancellation effects are expected.

Liebert et al. (2003) have found that the incidence of magnetism at the level of ~ 2 MG or greater is at least $\sim 10\%$, or higher. They suggest that the

total fraction of magnetic WDs may be substantially higher than 10% due to the limited spectropolarimetric analyses capable of detecting lower field strengths down to ~ 10 kG. Our 3 detections out of 12 objects seem to indicate that low magnetic fields on WDs (<10 kG) are frequent while high magnetic fields are relatively rare. However, with only three detections this hypothesis remains insecure. If confirmed by future observations, the investigation of weak magnetic fields in WDs could form a cornerstone for the future investigation of the properties and evolution of stellar magnetic fields.

Our sample of WDs is too small to discuss in detail the dependence of the magnetic field strength on the stellar parameters (masses and cooling ages). However, two of our detections (WD 0446–789 and WD 1105–048) have masses of $0.5 M_{\odot}$. This means that their progenitors on the main-sequence had less than $1 M_{\odot}$ (Weidemann 2000). These two stars are therefore very different from the majority of WDs with MG magnetic fields which tend to have higher masses (Greenstein & Oke 1982; Liebert 1988) and, therefore, high-mass parent stars.

At our signal-to-noise ratio, magnetic fields down to about 2 kG can be measured. There is still the possibility that all magnetic WDs contain surface magnetic fields at the 1 kG level. To test this hypothesis, much longer exposure times would be necessary, even with the VLT. Full details of our analysis can be found in Aznar Cuadrado et al. (2004).

References

- Aznar Cuadrado, R., Jordan, S., Napiwotzki, R., Schmid, H. M., Solanki, S. K., & Mathys, G. 2004, *A&A*, 423, 1081
- Benvenuto, O. G., & Althaus, L. G. 1999, *MNRAS*, 303, 30
- Bergeron, P., Wesemael, F., & Beauchamp, A. 1995, *PASP*, 107, 1047
- Casini, R., & Landi degl'Innocenti E. 1994, *A&A*, 291, 668
- Fabrika, S. N., Valyavin, G. G., & Burlakova, T. E. 2003, *Astronomy Letters*, 29, 737
- Greenstein, J. L., & Oke, J. B. 1982, *ApJ*, 252, 285
- Kemp, J. C., Swedlund, J. B., Landstreet, J. D., & Angel, J. R. P. 1970, *ApJ*, 161, L77
- Landi degl'Innocenti, E., & Landi degl'Innocenti, M. 1973, *Solar Phys.*, 29, 287
- Landstreet, J. D. 1982, *ApJ*, 258, 639
- Liebert, J. 1988, *PASP*, 100, 1302
- Liebert, J., Bergeron, P., & Holberg, J. B. 2003, *AJ*, 125, 348
- Mathys, G. 2001, in *ASP Conf. Ser. Vol. 248, Magnetic Fields Across the Hertzsprung-Russell Diagram*, ed. G. Mathys, S. K. Solanki, & D. T. Wickramasinghe, (San Francisco: ASP), 267
- Napiwotzki, R., Green, P. J., & Saffer, R. A. 1999, *ApJ*, 517, 399
- Napiwotzki, R., Christlieb, N., Drechsel, H., et al. 2003, *ESO-Messenger*, 112, 25
- Rüedi, I., Solanki, S. K., Mathys, G., & Saar, S. H. 1997, *A&A*, 318, 429
- Saar, S. H. 1996, in *IAU Colloquium 153, Magnetodynamic Phenomena in the Solar Atmosphere - Prototypes of Stellar Magnetic Activity*, ed. Y. Uchida, T. Kosugi, & H. S. Hudson, (Dordrecht: Kluwer), 367
- Schmidt, G. D., & Smith, P. S. 1995, *ApJ*, 448, 305
- Schmidt, G. D., Harris, H. C., Liebert, J., Eisenstein, D. J., et al. 2003, *ApJ*, 595, 1101
- Weidemann, V. 2000, *A&A*, 363, 647
- Werner, K. 1986, *A&A*, 161, 177